HOSTED BY
ELSEVIER

Contents lists available at ScienceDirect

Asian Pacific Journal of Tropical Medicine

journal homepage: http://ees.elsevier.com/apjtm

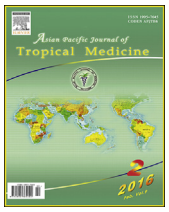

Original research http://dx.doi.org/10.1016/j.apjtm.2016.01.002

Correlation between blood circulation grading and angiogenesis using ultrasonic contrast of rabbit VX2 hepatic carcinoma

Chang-Song Xu[1], Yi-Jin Su[2], Ming Xu[1], Wei Liu[1], Peng Hao[1], Lian-Fang Du[2*]

[1]*Department of Medical Ultrasonics, the Affiliated Huai'an No.1 People's Hospital of Nanjing Medical University, Huai'an 223300, China*

[2]*Department of Medical Ultrasonics, the Affiliated Shanghai No.1 People's Hospital of Nanjing Medical University, Shanghai 200080, China*

ARTICLE INFO

Article history:
Received 15 Nov 2015
Received in revised form 20 Dec 2015
Available online 11 Jan 2016

Keywords:
Hepatic carcinoma
VX2
Ultrasonic contrast
Angiogenesis
bFGF
TNF-α

ABSTRACT

Objective: To build the rabbit model of VX2 hepatic carcinoma, examine the tumor body using the ultrasonic contrast and study the correlation between the blood circulation grading and angiogenesis.

Methods: The VX2 tumor strain was prepared in the lateral muscle of the hind legs of 40 male New Zealand rabbits (which were purchased from Nanjing Senbao Biotech Co., Ltd.). The tumor block was embedded in the center of left liver lobe directly to build the rabbit model of VX2 hepatic carcinoma. The ultrasonic contrast was performed 14 d after implanting the tumor body. The semi-quantitative classification (0–IV level) was taken according to the blood flow of tumor vessel. Animals were executed using the air embolism method. The liver was separated to extract RNA and total protein respectively. The real-time PCR and western blotting method were employed to detect the expression of angiogenesis-related factors of VEGF, bFGF and TNF-α, while the ultrasonic contrast to detect the correlation with blood circulation grading. The Pearson product moment correlation coefficient was used to measure the linear relationship between these two variables and analyze the correlation between the blood circulation grading and angiogenesis using the ultrasonic contrast.

Results: Thirty-three rabbits had the successful model of VX2 hepatic carcinoma. The blood circulation grading by ultrasonic contrast was: 2 cases at level 0 (6.60%), 5 cases at level I (16.7%), 12 cases at level II (40.0%), 6 cases at level III (20.0%) (local dense or clustered blood flow) and 5 cases at level IV (16.7%). The results showed that there was positive correlation between three angiogenesis-related factors and the blood circulation grading. The correlation coefficient between three angiogenesis-related factors and the blood circulation grading was over 0.9, which indicated the relatively high correlation.

Conclusions: The ultrasound blood circulation grading for the hepatic carcinoma can clearly reflect the changes of blood vessel, which will be of critical significance for the early diagnosis of hepatic carcinoma and clinical evaluation of angiogenesis indicators.

1. Introduction

The hepatic carcinoma is one of common malignant tumors, but its exact molecular mechanism has not been clear yet. Because of the insidious clinical symptoms, patients were always diagnosed at the middle and advanced stage, with extremely poor prognosis [1,2]. Accordingly, the research on the pathogenesis of hepatic carcinoma will be of clinical significance to promote the early diagnosis and estimation of prognosis. For the pathogenesis of primary hepatic carcinoma, the current findings regarded it as the complicated process involving many factors and many procedures, as the result of genetic and environmental factors [3]. The growth and metastasis of hepatic carcinoma cells are closely related to the angiogenesis of tumor. The new blood vessel and inhibitory factor are involved in the regulation of angiogenic switch of

*Corresponding author: Lian-Fang Du, Department of Medical Ultrasonics, the Affiliated Shanghai No.1 People's Hospital of Nanjing Medical University, Shanghai 200080, China.
Tel: +86 13861678770
E-mail: lianfangdu1982@163.com

Peer review under responsibility of Hainan Medical College.
Foundation project: It was supported by the National Natural Science Foundation of China (Protect No. 81502047).

1995-7645/Copyright © 2016 Hainan Medical College. Production and hosting by Elsevier B.V. This is an open access article under the CC BY-NC-ND license (http://creativecommons.org/licenses/by-nc-nd/4.0/).

hepatic carcinoma to generate the inhibitory factor using its unique properties, which are the major positive regulators in the angiogenesis of tumor. The vascular endothelial growth factor (VEGF) and basic fibroblast growth factor (bFGF) were regarded as two important pro-angiogenic factors [4,5], which could reflect the quantitative indicators of angiogenesis, while its expression was closely related to the prognosis of tumor.

The ultrasonic contrast is also known as the acoustic contrast, as the new technique applied in the clinical practice in recent years. By injecting the contrast agent, it was capable to dynamically and clearly show the micro-vessels. Especially, the new imaging technique for the blood vessel of tumor could significantly improve the differentiation, sensibility and specificity of ultrasound diagnosis [6,7]. As some kind of functional imaging technique, the ultrasonic contrast possesses many advantages that the normal ultrasonography does not have. In the present clinical practice, such technique is mainly applied in the diagnosis of hepatic lesions. According to the time after the injection of contrast agent, the imaging of liver can be divided into the arterial phase, portal phase and late phase. Besides, the specific diagnosis is performed on the lesions according to the mode of entry and exit of contrast agent in the lesions during the different phases, namely the different speed, mode and strength.

In this study, the ultrasonic contrast technique was employed to detect the patterns of blood flow in the tumor. Besides, the real-time PCR and western blotting were employed to detect the correlation between the expression of angiogenesis-related factors of VEGF, bFGF and tumor necrosis factor alpha (TNF-α) and the blood circulation grading measured by the ultrasonic contrast.

2. Materials and methods

2.1. Materials

2.1.1. Laboratory animals and cells

Forty male New Zealand rabbits with the weight of (2.5 ± 0.5) kg and age of (4–5) months were purchased from Shanghai SLAC Laboratory Animal Co., Ltd. All laboratory animals were given the standard diet and clean water freely during the experiment. The ventilation was good in the feeding room, with the natural lighting day and night. The culture temperature was maintained at (18–25) °C.

The rabbit's anaplastic squamous VX2 carcinoma cell lines were purchased from Shanghai Biochemical Reagent Fusheng Co., Ltd. and stored in the liquid nitrogen in this laboratory.

2.1.2. Main reagents and instruments

The ultrasonic contrast agent was purchased from Bracco-SonoVue; the protein extraction-RIPA lysis buffer from Wuhan Boster Biological Technology, Ltd. (AR0105); RNA extraction kit from Bioteke (RP55011); the reverse transcription kit cDNA Synthesis from HiScript (R111-01); real-time fluorescent quantitative PCR from Bio-Rad (172-5264); VEGF monoclonal antibody from Santa Cruz Biotechnology (sc-48835); bFGF monoclonal antibody from Santa Cruz Biotechnology (136255), TNF-α monoclonal antibody from Santa Cruz Biotechnology (374186); GAPDH monoclonal antibody from Santa Cruz Biotechnology (365062); horseradish peroxidase-labeled secondary antibody from Beijing Zhongshan Jinqiao Biotechnology; PVDF film from Millipore (0.2 μm); and ECL Chemiluminescent Substrate Reagent Kit from Life Technologies (America, item No. WP20005).

DNA/RNA analyzer was Bio-Rad ChemiDoc™ XRS+; CO_2 cell culture incubator was Thermo Scientific Series 8000; the fluorescent quantitative PCR system was Lightcycler480II; and the color Doppler ultrasonic diagnostic apparatus was Siemens S2000.

2.2. Methods

2.2.1. Building of animal model

VX2 cells were taken out from the liquid nitrogen for the resuscitation and subculture. The cell suspension was then prepared (the cell concentration was adjusted to about 10^7 pieces/mL). The precooled cell suspension was taken by 2 mL to be injected into the lateral muscle of the rabbit's hind legs. After 14 d, the ophthalmic scissors were used to scissor the peripheral tissue of tumor and PBS suspension. Rabbits were anesthetized using 30 mg/kg sodium pentobarbital and then fixed at the prone position. The rabbits' skin and subcutaneous tissue were separated to expose the lower edge of the left liver lobe. The ophthalmic scissors were used to scissor the small incision about 3 mm long at the position with the thick tissue. The prepared tumor block was then implanted in the tissue. The incision was stuffed with the gelatin sponge. After the hemostasis by compression, 400 000 units of antibiotic were injected into the muscle [10,11].

2.2.2. Ultrasonic contrast

The ultrasonic probe 9L4 (Siemens) was adopted to observe and record the size of liver tumor and the inside and edge of lesion. After the two dimensional Doppler flow imaging, then the two dimensional ultrasonic contrast imaging was performed. Five mL 0.9% NaCl solution was added in SonoVue lyophilized powder and it was then shaken hard to prepare the sulfur hexafluoride microbubble suspension. The contrast agent (phospholipid microencapsulation of sulfur hexafluoride) was injected in the auricular vein with the dose of 0.15 mL/kg, which was then washed with 1.5 mL 0.9% NaCl. The signaling process of blood flow was observed under the real-time and dynamic gray status and the dynamic contrast images were saved. The mechanical index was regulated to 0.15. The SonoLiverR CAP quantitative analysis software was employed for the analysis of parameters. The semi-quantitative classification of blood flow (level 0–IV) were: Level 0: no significant signal of blood flow; level I: few dotted or short line-like blood flow; level II: rich blood supply with the long line-like or branched blood flow; level III: local dense or clustered blood flow; level IV: mass-like or diffusely distributed blood flow [8,9].

2.2.3. Real-time PCR [11]

The UV spectrophotometer was adopted to detect A260 and concentration of RNA solution, using the ratio of OD_{260}/OD_{280} to evaluate the purity of RNA. The total RNA was reversely transcripted to cDNA following the instruction manual of reverse transcription kit. The real-time PCR was employed to detect the expression of related genes. The mRNA sequence of *E-cadherin*, *Vimentin*, *β-catenin* and *CyclinD1* genes could be referred to NCBI database and then the real-time PCR primers could be designed. All primers were synthesized by SBS

Genetech Co., Ltd.. Ct value of each gene amplification was detected, where Ct value was negatively correlated to the starting copy number. The double △Ct method was adopted to calculate the relative expression of target gene. The concentration of primers in PCR system was (350–400) nM and cDNA template as 150 ng. The reaction conditions included the predenaturation at 95 °C for 10 min, denaturation at 95 °C for 10 s, annealing temperature was set according to the primer Tm for 20sec and extension at 72 °C for 33 s, with 40 cycles in total.

2.2.4. Western blotting

The collected tissues were ground in the liquid nitrogen. Samples were lysed by the protein extraction kit, with the addition of protease inhibitor cocktail. After being put on the ice for 30 min, the probe-type ultrasound was used to produce the short impact with the appropriate frequency on the ice. The lysis mixture was centrifuged at 4 °C and 13 000 r/min for 20 min. The supernatant was transferred to the new centrifuge tube. Protein Assay Kit was employed to detect the protein concentration.

SDS-PAGE electrophoresis was performed on protein samples. The gel was soaked in the transfer buffer for 10 min of equilibrium. It was installed with the transfer 'sandwich' with 100 V and (45–60) min. After the transfer, PVDF film was washed with TBS for (10–15) min. The film was placed in TBS/T blocking buffer containing 5% (w/v) skimmed milk powder and shaken at the room temperature for 1 h. Then the primary antibody with the appropriate degree of dilution was added [diluted with TBST containing 1% (w/v) skimmed milk powder]. It was incubated at the room temperature for 2 h and then the film was washed with TBST for 3 times, (5–10) min every time. The film was incubated with the secondary antibody (1:10 000, horseradish peroxidase-labeled) that was diluted with TBST containing 0.05% (w/v) skimmed milk powder. It was incubated at the room temperature for 1 h and then the film was washed with TBST for 3 times, (5–10) min every time. It was exposed and then photographed to save the experimental results. The experiment was repeated three times. Quantity one v4.62 was used to measure the gray value of molecular band (trace tracking). The optical density curve could be drawn according to the optical density of different electrophoretic bands. The area under the curve of optical density was then calculated as the quantitative basis of electrophoretic bands. The statistical analysis was performed as well.

2.3. Statistical analysis

The experimental data was treated with SPSS16.0. The measurement data was expressed by mean ± SD. The *t* test was employed for the comparison between groups. Pearson correlation coefficient of Minitab was adopted for the correlation analysis. $P < 0.05$ indicated the statistical difference.

3. Results

3.1. Building of animal model

Forty laboratory rabbits were randomly divided into two groups, with 5 rabbits in the control group and 35 ones in the model group. Two rabbits in the model group died because of infection during the modeling. Thirty-three rabbits had the successful modeling, with the success rate of 94.3%.

According to the results of two-dimensional ultrasonic testing on the liver of rabbits, the liver of animals in the normal control group had the regular shape, clear boundary and even optical distribution; while the liver of animals in the model group mainly had the round solid masses, showing the calcified lesions with the strong echo. After the ultrasonic contrast testing, the liver tissue was taken for HE staining. Cells in the normal area of liver tissue had the compact arrangement, with the clear boundary to the adjacent liver lobule. For the liver in the model group, according to the sections, the boundary of nucleus was fuzzy, with the broken fibrous tissue around.

3.2. Ultrasonic contrast analysis and blood circulation grading

The two dimensional ultrasonic test found 30 hepatic carcinoma lesions in 33 model rabbits, with the round or oval echo in the left liver lobe. Where 8 lesions had the fuzzy boundary and the mean volume of all lesions was (23.8 ± 3.3) cm^3 (the volume of tumor body V = 1/2 ab^2, where was the max diameter and b was the min diameter). The ultrasonic contrast testing detected 30 lesions in total, with the volume of (25.6 ± 2.1) cm^3. All lesions could clearly show the boundary between the tumor nodules and the surrounding normal liver tissue. The contrast agent (phospholipid microencapsulation of sulfur hexafluoride) was injected in the auricular vein with the dose of 0.15 mL/kg, which was then washed with 1.5 mL 0.9% NaCl. The signaling process of blood flow was observed under the real-time and dynamic gray status. Four seconds after injecting the contrast agent, the whole tumor showed the high enhancement during the arterial phase, with the dissension and low enhancement during the portal phase, which could detect the typical contrast mode of malignant tumor, namely 'fast in and fast out'.

The SonoLiverR CAP quantitative analysis software was employed for the analysis of parameters, while the motion compensation mode for the appropriate compensation to reduce the error. According to the results of ultrasonic contrast, there was the significant difference in the quantitative indices of ultrasonic contrast, such as the ascending slope, arrival time, time-to-peak, peak intensity and area under curve between the hepatic carcinoma tissue and surrounding normal liver tissue ($P < 0.05$) (Table 1).

The ultrasonic contrast technique was employed to detect the pattern of blood flow and abundance of blood supply of 30 tumor bodies, with the blood circulation grading of 2 cases at level 0 (no obvious signal of blood flow) (0.60%), 5 cases at level I (few dotted or short line-like blood flow) (16.7%), 12 cases at level II (rich blood supply with the long line-like or branched blood flow) (40.0%), 6 cases at level III (local dense or clustered blood flow) (20.0%) and 5 cases at level IV (mass-like or diffusely distributed blood flow) (16.7%).

3.3. Expression of angiogenesis-related factors

3.3.1. Expression of related genes detected by real-time PCR

The grouping was done according to the blood circulation grading of ultrasonic contrast, while real-time PCR was employed to detect the expression of related genes in the liver

Table 1
Comparison of quantitative indices of ultrasonic contrast between hepatic carcinoma tissue and surrounding normal liver tissue.

	AS	AT(s)	TTP(s)	PI	AUC
Tumor-like lesion	4.96 ± 1.13	6.32 ± 0.09	9.26 ± 1.06	26.33 ± 2.22	189.63 ± 100.52
Surrounding tissue	0.94 ± 0.99	10.30 ± 0.66	18.39 ± 0.85	15.38 ± 0.38	165.33 ± 99.39
t	5.52	9.31	40.23	26.01	0.97
P	>0.05	<0.01	<0.01	<0.01	>0.05

AS: ascending slope; AT: arrival time; TP: time-to-peak; PI: peak intensity; AUC: area under curve.

tissue. Taking level 0 as the control group (namely the relative expression as 1), the expression of angiogenesis-related factors of *VEGF*, *bFGF* and *TNF-α* from level I to IV was shown in Table 2. It could be indicated that there was the positive correlation between three angiogenesis-related factors and blood circulation grading.

3.3.2. Expression of related factors detected by western blotting

After extracting the total protein from the tissue, the expression of angiogenesis factors was tested at the protein level. The western blotting assay was performed to detect the expression of related molecules in the total protein of liver tissue. Quantity one v4.62 was used to measure the gray value of molecular band (trace tracking). The optical density curve could be drawn according to the optical density of different electrophoretic bands. The area under the curve of optical density was then calculated as the quantitative basis of electrophoretic bands (Table 3). According to the results, the expression trend of three angiogenesis-related factors was in accordance with the findings of real-time PCR.

3.4. Correlation analysis

To study the correlation between the blood circulation grading and angiogenesis using the ultrasonic contrast of hepatic carcinoma, the relative expression of three factors at each blood circulation grading was analyzed (real-time PCR). Besides, Minitab15 was employed for the correlation analysis (with the vertical axis as the blood circulation grading and horizontal axis as the mean of relative expression), with the results shown in Table 4. The correlation coefficient between three angiogenesis-related factors and blood circulation grading was all over 0.9, which indicated the high correlation. Especially, the expression of *bFGF* was related to the grading level.

Table 2
Expression of related genes detected by real-time PCR (Mean ± SD).

Grading	Gene		
	VEGF	*bFGF*	*TNF-α*
I	1.72 ± 0.21	1.31 ± 0.16	1.35 ± 0.21
II	2.23 ± 0.34	1.89 ± 0.22	2.76 ± 0.33
III	5.74 ± 0.35	2.58 ± 0.14	2.84 ± 0.27
IV	8.93 ± 0.16	3.06 ± 0.11	3.19 ± 0.16

Table 3
Expression and relative quantification of related genes detected by WB (Mean ± SD).

Grading	Gene		
	VEGF	*bFGF*	*TNF-α*
0	0.73 ± 0.02	0.96 ± 0.03	0.21 ± 0.09
I	1.25 ± 0.18	0.76 ± 0.16	0.36 ± 0.18
II	1.29 ± 0.33	0.98 ± 0.21	0.41 ± 0.06
III	1.37 ± 0.22	0.89 ± 0.13	0.54 ± 0.09
IV	1.39 ± 0.16	1.09 ± 0.06	0.66 ± 0.08

Table 4
Correlation between blood circulation grading and angiogenesis detected by ultrasonic contrast.

Blood circulation grading	*n*	Relative expression of genes (Mean ± SD)		
		VEGF	*bFGF*	*TNF-α*
0	2	1.00 ± 0.11	1.00 ± 0.21	1.00 ± 0.08
I	5	1.72 ± 0.21	1.31 ± 0.16	1.35 ± 0.21
II	12	2.23 ± 0.34	1.89 ± 0.22	2.76 ± 0.33
III	6	5.74 ± 0.35	2.58 ± 0.14	2.84 ± 0.27
IV	5	8.93 ± 0.16	3.06 ± 0.11	3.19 ± 0.16

4. Discussion

The hepatic carcinoma is the third most common malignant tumor with the mortality after gastric carcinoma and esophagus cancer. Because of the abundant blood circulation in the liver, it becomes the most common malignant tumor and the hepatic carcinoma has the poor prognosis and high mortality. The occurrence and development of tumor are always the result of long-term accumulation of many factors. Though the 'three-step' for the hepatic carcinoma, namely the hepatitis-liver cirrhosis-hepatic carcinoma, had been widely acknowledged [12], the molecular mechanism for each process has still not been clear yet. The animal model of diseases is the important tool for the human being to study the malignant tumor. The implantation model of rabbit hepatic carcinoma VX2 is characterized by the easy building, short experimental period, high success rate and good repeatability. Besides, because the invasion of VX2 tumor cells is similar with the primary huge hepatocellular carcinoma of human, it is modeled as the hypervascular tumor. As the largest laboratory animal model of hepatic carcinoma, the rabbit model of VX2 hepatic carcinoma has been widely applied in the studies of hepatic carcinoma [13–15]. During the modeling, considering that the right liver lobe of rabbit was smaller than the left one and the left hepatic artery was relatively thick and convenient for the operation, the tumor tissue was implanted in the left liver lobe during the modeling of VX2 hepatic carcinoma. The previous researches indicated that the rabbit VX2 tumor could be implanted in the internal organs such as the subcutaneous tissue, muscle, liver and kidney, showing the high success rate especially for the implantation in the liver, which would thus provide the important tool for the treatment of hepatic carcinoma and the studies in the imaging of hepatic carcinoma.

The ultrasonic contrast is the new technique applied in the clinical practice in recent years. By injecting the contrast agent,

it was capable to dynamically and clearly show the microvessels. Especially, the new imaging technique for the blood vessel of tumor could significantly improve the differentiation, sensibility and specificity of ultrasound diagnosis [6,7,16]. The ultrasonic contrast technique has become the sophisticated tool in the diagnosis and treatment of hepatic carcinoma. Generally, the space occupying lesions would be found on the conventional ultrasonic instrument at first. After injecting the ultrasonic contrast agent through the peripheral vein, it could thus observe the enhancement of space occupying inside the liver. Because of the difference between the characteristics of blood supply of malignant tumor and the benign lesions, the difference in the ultrasound enhancement could be used for the diagnosis and differential identification of malignant hepatic tumor. With the great progress in the ultrasonic contrast technique in recent years, its clinical value, especially in the diagnosis and treatment of tumors, has aroused people's attention. The diagnostic capacity of acoustic contrast is better or has the same sensitivity as the helical CT at least. The microbubble is recognized as the best contrast agent in the human microvessel because of its strong echo reflection performance, which can reflect the blood perfusion of organs and also does not interfere with the hemodynamics [17–19].

The ultrasonic contrast technique was employed to detect the pattern of blood flow and abundance of blood supply of tumor bodies, with the blood circulation grading (level 0–IV): Level 0: no significant signal of blood flow; level I: few dotted or short line-like blood flow; level II: rich blood supply with the long line-like or branched blood flow; level III: local dense or clustered blood flow; level IV: mass-like or diffusely distributed blood flow. The real-time PCR and western blotting were employed to detect the correlation between the expression of angiogenesis-related factors of *VEGF*, *bFGF* and *TNF-α* and the blood circulation grading measured by the ultrasonic contrast.

The expression of angiogenesis-related factors of *VEGF*, *bFGF* and *TNF-α* from level I to IV indicated that there was the positive correlation between three angiogenesis-related factors and blood circulation grading. The results of testing at the protein level were in accordance with ones of real-time PCR. Minitab15 was employed for the correlation analysis (with the vertical axis as the blood circulation grading and horizontal axis as the mean of relative expression). According to the results, the data fitting was good and the correlation coefficient between three angiogenesis-related factors and the blood circulation grading was over 0.9, which indicated the relatively high correlation. Especially, the expression of *bFGF* was highly correlated with the grading.

Conflict of interest statement

We declare that we have no conflict of interest.

References

[1] Roayaie K, Roayaie S. Liver transplant for hepatocellular cancer: very small tumors, very large tumors, and waiting time. *Clin Liver Dis* 2014; **18**(3): 603-612.

[2] Berlakovich GA. Challenges in transplantation for alcoholic liver disease. *World J Gastroenterol* 2014; **20**(25): 8033-8039.

[3] Wang T, Li C, Liu Y, Li T, Zhang J, Sun Y. Inhibition effects of Chinese cabbage powder on aflatoxin B1-induced liver cancer. *Food Chem* 2015; **186**: 13-19.

[4] Engels EA, Jennings L, Kemp TJ, Chaturvedi AK, Pinto LA, Pfeiffer RM, et al. Circulating TGF-β1 and VEGF and risk of cancer among liver transplant recipients. *Cancer Med* 2015; **4**(8): 1252-1257.

[5] Wang JH, Liu N, Du HW, Weng JS, Chen RH, Xiao YC, et al. Effects of adipose-derived stem cell transplantation on the angiogenesis and the expression of bFGF and VEGF in the brain post focal cerebral ischemia in rats. *Chin J Cell Mol Imunnol* 2008; **24**(10): 958-961.

[6] Joo I. The role of intraoperative ultrasonography in the diagnosis and management of focal hepatic lesions. *Ultrasonography* 2015; **34**: 246-257.

[7] Chiorean L, Schreiber-Dietrich D, Braden B, Cui XW, Buchhorn R, Chang JM, et al. Ultrasonographic imaging of inflammatory bowel disease in pediatric patients. *World J Gastroenterol* 2015; **21**(17): 5231-5241.

[8] Yen PL, Wu HK, Tseng HS, Kuo SJ, Huang YL, Chen HT, et al. Vascular morphologic information of three-dimensional power doppler ultrasound is valuable in the classification of breast lesions. *Clin Imaging* 2012; **36**(4): 267-271.

[9] Kachewar SG, Gandage SG. A classification of patterns of fetal middle cerebral artery velocity waveforms as seen on Doppler ultrasound. *Jpn J Radiol* 2012; **30**(7): 582-588.

[10] Tanaka K, Maeda N, Osuga K, Higashi Y, Hayashi A, Hori Y, et al. *In vivo* evaluation of irinotecan-loaded quadrasphere microspheres for use in chemoembolization of VX2 liver tumors. *J Vasc Interv Radiol* 2014; **25**(17): 1727-1735.

[11] Livak KJ, Schmittgen TD. Analysis of relative gene expression data using real-time quantitative PCR and the $2^{-\triangle\triangle CT}$ method. *Methods* 2001; **25**(4): 402-408.

[12] Karlsen TH, Lammert F, Thompson RJ. Genetics of liver disease: from pathophysiology to clinical practice. *J Hepatol* 2015; **62**(1S): S6-S14.

[13] Lee KC, Moon WK, Chung JW, Choi SH, Cho N, Cha JH, et al. Assessment of lymph node metastases by contrast-enhanced MR imaging in a head and neck cancer model. *Korean J Radiol* 2007; **8**(1): 9-14.

[14] Sonoda A, Nitta N, Nitta-Seko A, Ohta S, Nagatani Y, Mukaisho K, et al. Time-course studies of implanted rabbit VX2 liver tumors to identify the appropriate time for starting hepatic arterial embolization in animal models. *Oncology* 2011; **80**(1–2): 92-96.

[15] Wang Z, Yang G, Nie P, Fu J, Wang X, Liu D. Dynamical observation on biological progression of VX2 liver tumors to identify the optimal time for intervention in animal models. *PLoS One* 2013; **8**(8): e74327.

[16] Yoon JH, Cho A, Lee HS, Kim EK, Moon HJ, Kwak JY. Thyroid incidentalomas detected on (18)F-fluorodeoxyglucose-positron emission tomography/computed tomography: Thyroid Imaging Reporting and Data System (TIRADS) in the diagnosis and management of patients. *Surgery* 2015; **158**(5): 1314-1322.

[17] Natsuda K, Soyama A, Takatsuki M, Yamaguchi T, Torashima Y, Kitasato A, et al. Acoustic radiation force impulse elastography for liver disease staging in human immunodeficiency virus and hepatitis C virus co-infection. *Nihon Shokakibyo Gakkai Zasshi* 2014; **111**(4): 737-742.

[18] Mishima M, Toh U, Iwakuma N, Takenaka M, Furukawa M, Akagi Y. Evaluation of contrast Sonazoid-enhanced ultrasonography for the detection of hepatic metastases in breast cancer. *Breast Cancer* 2014; http://dx.doi.org/10.1007/s12282-014-0560-0.

[19] van Rijn RR, Nievelstein RA. Paediatric ultrasonography of the liver, hepatobiliary tract and pancreas. *Eur J Radiol* 2014; **83**(9): 1570-1581.